JOURNAL OF VIROLOGY, Nov. 1998, p. 8568–8577 Vol. 72, No. 11
0022-538X/98/$04.00+0

Circular Intermediates of Recombinant Adeno-Associated Virus Have Defined Structural Characteristics Responsible for Long-Term Episomal Persistence in Muscle Tissue

DONGSHENG DUAN, PRERNA SHARMA, JUSAN YANG, YONGPING YUE, LORITA DUDUS, YULONG ZHANG, KRISHNA J. FISHER, AND JOHN F. ENGELHARDT*

Department of Anatomy and Cell Biology and Department of Internal Medicine, University of Iowa Medical Center, Iowa City, Iowa

Received 20 May 1998/Accepted 16 July 1998

Adeno-associated viral (AAV) vectors have demonstrated great utility for long-term gene expression in muscle tissue. However, the mechanisms by which recombinant AAV (rAAV) genomes persist in muscle tissue remain unclear. Using a recombinant shuttle vector, we have demonstrated that circularized rAAV intermediates impart episomal persistence to rAAV genomes in muscle tissue. The majority of circular intermediates had a consistent head-to-tail configuration consisting of monomer genomes which slowly converted to large multimers of >12 kbp by 80 days postinfection. Importantly, long-term transgene expression was associated with prolonged (80-day) episomal persistence of these circular intermediates. Structural features of these circular intermediates responsible for increased persistence included a DNA element encompassing two viral inverted terminal repeats (ITRs) in a head-to-tail orientation, which confers a 10-fold increase in the stability of DNA following incorporation into plasmid-based vectors and transfection into HeLa cells. These studies suggest that certain structural characteristics of AAV circular intermediates may explain long-term episomal persistence with this vector. Such information may also aid in the development of nonviral gene delivery systems with increased efficiency.

Adeno-associated virus type 2 (AAV) contains a single-stranded DNA genome of approximately 4.7 kb with two characteristic inverted terminal repeats (ITRs). Replication of AAV requires an additional helper virus such as adenovirus or herpesvirus. In the absence of a helper virus, wild-type AAV (wtAAV) establishes a latent infection by integrating into the host genome in a site-specific manner at the AAVS1 locus on human chromosome 19 (21). Pivotal studies by Samulski and colleagues demonstrated that ITR sequences are sufficient for packaging of AAV genomes and paved the way for the generation of recombinant vectors (28, 29). In contrast to wtAAV, recombinant AAV (rAAV) vectors do not appear to preferentially integrate at AAVS1 loci. Rather, these recombinant vectors can persist as episomes (1, 13) or alternatively can integrate into the cellular genome at sites other than chromosome 19 AAVS1 (11, 18, 22, 26, 27, 35). To date, no concrete evidence has supported or disproved integration as the predominant mechanism of rAAV persistence in vivo.

Muscle-mediated gene transfer represents a very promising approach for the treatment of hereditary myopathies and several other metabolic disorders. Previous studies have demonstrated remarkably efficient and persistent transgene expression to skeletal muscle in vivo with rAAV vectors. Applications in this model system include the treatment of several inherited disorders such as factor IX deficiency in hemophilia B and erythropoietin deficiencies (15, 19). Although the conversion of low-molecular-weight AAV genomes to high-molecular-weight concatemers has been inferred as evidence for integration of proviral DNA in the host genome, no direct evidence exists in this regard (5, 10, 34). Furthermore, the molecular processes involved in establishing stable gene transduction in nondividing mature myofibers remains a mystery. In the present study, we examined whether stability of rAAV genomes in muscle might be conferred through the formation of circular intermediates. Circular intermediates have previously been hypothesized as preintegrating structures of AAV (22), but conclusive identification has not yet been documented. To this end, we sought to characterize the abundance and molecular structure of AAV circular intermediates in muscle tissue by using a rAAV shuttle vector capable of rescuing circular intermediates by bacterial transformation. This shuttle virus, called AV.GFP3ori contained a green fluorescence protein (GFP) reporter gene, an ampicillin resistance gene, and a bacterial origin of replication. These studies have demonstrated that head-to-tail episomal circularized monomer and concatemer genomes represent a predominant molecular structure of rAAV following in vivo delivery to muscle tissue. Furthermore, circular intermediates demonstrated sustained episomal persistence in muscle tissue as well as increased episomal stability in cell lines following liposome-mediated transfection. Taken together, our results suggest that in vivo persistence of rAAV can occur through episomal circularized genomes which may represent preintegration intermediates with increased episomal stability.

* Corresponding author. Mailing address: Department of Anatomy and Cell Biology, University of Iowa School of Medicine, 51 Newton Rd., Room 1-101 BSB, Iowa City, IA 52242. Phone: (319) 335-7753. Fax: (319) 335-7198. E-mail: john-engelhardt@uiowa.edu.

MATERIALS AND METHODS

Production of rAAV shuttle vector. The *cis*-acting plasmid (pCisAV.GFP3ori) used for rAAV production was generated by subcloning the *Bsp*120I/*Not*I fragment (743 bp) of the GFP transgene from pEGFP-1 (Clontech) between the cytomegalovirus (CMV) enhancer/promoter and simian virus 40 poly(A) site by blunt-end ligation. The CMV enhancer/promoter and simian virus 40 poly(A) sequences were derived from pcDNA3.1 (Invitrogen). A 2.5-kb cassette containing β-lactamase and bacterial replication origin from pUC19 was blunt-end ligated downstream of the GFP reporter cassette. The ITR elements were derived from pSub201 (29). The entire plasmid contains a 4.7-kbp AAV component flanked by a 2-kbp stuffer sequence which was derived from the luciferase gene of the pGL3-basic vector (Promega). The integrity of ITR sequences was confirmed by restriction analysis with *Sma*I and *Pvu*II and by direct sequencing using

TABLE 1. Control experiments for rescue of circular intermediates in bacteria

Type of input DNA	Source of DNA	No. of molecules (10^{10})	No. of ampicillin resistant bacterial colonies	Head-to-tail circular intermediates present?[e]
Purified rAAV	Hirt DNA from infected muscle (22 day)	3	$\sim 5 \times 10^3$	Yes
	Virus added to uninfected muscle Hirt DNA[a]	3	0	No
Linear ssDNA encompassing entire AAV genome[b]	Isolated from purified virus	3	2	No
Linear dsDNA encompassing entire rAAV genome	Isolated from proviral plasmid (*Hin*dIII/*Pvu*II)[c]	3	3	No
Linear dsDNA encompassing entire rAAV genome + ligase[d]	Isolated from proviral plasmid (*Hin*dIII/*Pvu*II)	3	$\sim 6 \times 10^3$	Yes

[a] Purified virus was added to muscle homogenates prior to preparation of Hirt DNA.

[b] Viral DNA predominantly contained single-stranded DNA (ssDNA) genomes, as evident by Southern blot analysis with the ITR probe (data not shown). However, there was also a small amount of double-stranded DNA (dsDNA) AAV genomes, likely due to reannealing of single-stranded genomes during preparation. Purified viral DNA concentrations were determined by optical density at 260 nm, and 75 ng, representing approximately 3×10^{10} viral genomes, was used for transformation of bacteria.

[c] *Hin*dIII/*Pvu*II digestion was used to remove the entire rAAV genome from pCisAV.GFP3ori. *Hin*dIII and *Pvu*II leave 10 and 0 bp of flanking sequence outside the 5′ and 3′ ITRs, respectively. The linear dsDNA fragment (4.7 kbp) was gel isolated following blunting with T4 DNA polymerase, and the DNA concentration was determined by optical density at 260 nm; 150 ng of linear fragment, representing approximately 3×10^{10} viral genomes, was used for transformation of bacteria.

[d] Linear dsDNA viral genomes (*Hin*dIII/*Pvu*II-blunted fragment) were treated with T4 DNA ligase prior to transformation of bacteria.

[e] Confirmed by restriction enzyme (*Ase*I, *Pst*I, and *Sph*I) digestion and Southern blotting against the ITR probe.

a modified dideoxy procedure which allowed for complete sequence through both 5′ and 3′ ITRs. rAAV stocks were generated by cotransfection of pCisAV.GFP3ori and pRep/Cap (9) together with coinfection of recombinant Ad.CMVlacZ (9) in 293 cells. The rAV.GFP3ori virus was subsequently purified through three rounds of CsCl banding as previously described (7). The typical yields from this viral preparation were 10^{12} DNA molecules/ml. DNA titers were determined by viral DNA slot blot hybridization against GFP P^{32}-labeled probe with copy number plasmid standards. The absence of helper adenovirus was confirmed by histochemical staining of rAAV-infected 293 cells for β-galactosidase, and no recombinant adenovirus was found in 10^{10} particles of purified rAAV stocks. The absence of significant wtAAV contamination was confirmed by immunocytochemical staining of AV.GFP3ori-Ad.CMVlacZ-coinfected 293 cells with anti-Rep antibodies. Transfection with pRep/Cap was used to confirm the specificity of immunocytochemical staining. No immunoreactive Rep staining was observed in 293 cells infected with 10^{10} rAAV particles.

Isolation of AAV circular intermediates from muscle tissue. The tibialis anterior muscles of 4- to 5-week-old C57BL/6 mice were infected with AV.GFP3ori (3×10^{10} particles) in HEPES-buffered saline (30 μl). Animal care was carried out in accordance with institutional guidelines of the University of Iowa. GFP expression was analyzed by direct immunofluorescence of freshly excised tissues and/or in formalin-fixed cryopreserved tissue sections in four independently injected muscles harvested at 0, 5, 10, 16, 22, and 80 days postinfection. Tissue sections were counterstained with propidium iodide to identify nuclear DNA. Muscle Hirt DNA was prepared according to a previously published protocol (16), with several modifications. Specifically, 50 mg of muscle tissue was chopped into small pieces and freeze-thawed three times in a dry ice–2-methylbutane bath. The sample was subsequently homogenized in 600 μl of buffer containing 10 mM Tris, (pH 8.0), 10 mM EDTA, 1% sodium dodecyl sulfate, and 1 μl of RNase (DNase free; 10-mg/ml stock; Boehringer Mannheim Biochemicals). After 30 min of incubation at 37°C, Pronase (Sigma catalog no. P0652) and proteinase K (Boehringer Mannheim catalog no. 745723) were added to final concentrations of 0.5 and 1 mg/ml, respectively. The reaction was continued for 120 min at 37°C, after which NaCl was added to a final concentration of 1.1 M. Following overnight precipitation at 4°C, samples were spun at 14,000 rpm in a tabletop microcentrifuge for 20 min, and low-molecular-weight Hirt DNA was purified from the supernatant by standard phenol-chloroform extraction (twice), chloroform extraction (twice), and ethanol precipitation. The final DNA pellet was resuspended in 20 μl of water.

Hirt DNA was isolated from at least three independent muscle specimens for each time point and used to transform *Escherichia coli* SURE cells, using 3 μl of Hirt DNA with 40 μl of electrocompetent bacterial ($\sim 10^9$ CFU/μg of DNA; Stratagene Inc.). The resultant total number of bacterial colonies was quantified for each time point; the abundance of head-to-tail circular intermediates was evaluated for each time point (>20 bacterial clones analyzed) by *Pst*I, *Ase*I, *Sph*I, and *Pst*I/*Ase*I digestion and confirmed by Southern blot analysis using ITR, GFP, and stuffer probes. The head-to-tail configurations in typical clones were also confirmed by dideoxy sequencing using primers EL118 (5′-CGGGGGTCGTTG GGCGGTCA-3′) and EL230 (5′-GGGCGGAGCCTATGGAAAA-3′), which are nested to 5′ and 3′ ITR sequences, respectively. Zero-hour controls were generated by mixing 3×10^{10} particles of AV.GFP3ori with control uninfected muscle lysates prior to Hirt DNA preparation. As described in Table 1, a number of additional controls were performed to rule out nonspecific recombination of linear AAV genomes in bacteria as a source for isolated circular intermediates.

Fractionation of muscle Hirt DNA preparations. Preparative-scale fractionation of the muscle Hirt DNA was performed by 1% agarose gel electrophoresis using a Bio-Rad Mini Prep Cell (catalog no. 170-2908). A 4.5-ml (10.5-cm) tubular gel containing 1× Tris-borate-EDTA buffer was poured according to the manufacturer's specification. A total of 20 μl of Hirt preparation from one entire muscle sample was loaded on top of the gel. Electrophoresis was carried out at a constant current of 10 mA over a period of 5 h. Sample eluent was drawn from the preparative gel apparatus by a peristaltic pump at a rate of 100 μl/min and eluted into a fraction collector at 250 μl/fraction. The collected DNA was subsequently concentrated by standard ethanol precipitation and used to transform *E. coli* SURE cells by electroporation as described above. Fractions were sized according to the migration of linear double-stranded DNA standards under identical gel running conditions. At least 10 clones were analyzed for each fraction by restriction digestion and Southern blotting to confirm the percentage of head-to-tail structures. Subsequently, the data from various fractions were grouped into size ranges as indicated in Fig. 4 (greater than 50 clones analyzed for structure from each size range and muscle sample).

In vitro persistence of AAV circular intermediates. Transgene expression and persistence of AAV circular intermediate plasmid clones were evaluated following transient transfection in HeLa and 293 cells. Two monomer circular intermediates, p81 and p87, which were structurally identical, by sequence and Southern blot criteria, to p139 (Fig. 3; isolated from muscle tissue at 22 days postinfection) were evaluated. However, p81 and p87 were originally isolated from AV.GFP3ori-infected HeLa cells. Subconfluent monolayers of cells in 24-well dishes were transfected with 0.5 μg of either an AAV circular intermediate (p81 or p87) or pCMVGFP, using Lipofectamine (Gibco BRL Inc.). The cultures were then incubated for 5 h in serum-free Dulbecco modified Eagle medium followed by incubation in Dulbecco modified Eagle medium supplemented with 10% fetal bovine serum. All plasmid DNA samples used for transfections were spiked with pRSVlacZ (0.5 μg) as an internal control for transfection efficiency. At 48 h posttransfection, cells were passaged at a 1:10 dilution and allowed to grow to confluency (day 5), at which time GFP clones were quantified for size and abundance by direct fluorescence microscopy. The percentage of β-galactosidase-expressing cells was also quantified at this time point by 5-bromo-4-chloro-3-indolyl-β-D-galactopyranoside (X-Gal) staining. At 5 days, cells were passaged an additional time (1:15 dilution); GFP clones were quantified again at day 10. The persistence of plasmid DNA at passage 5, 7, and 10 posttransfection was evaluated by Southern blot analysis of total cellular DNA using ^{32}P-labeled GFP probes. To determine whether the head-to-tail ITR array within circular intermediates was responsible for increases in the persistence of GFP expression, the head-to-tail ITR DNA element was subcloned into the luciferase plasmid pGL3 to generate pGL3(ITR). The head-to-tail ITR DNA element was isolated from a monomer circular intermediate (p81) by *Aat*II and *Hae*II double digestion and subsequently inserted into the *Sal*I site of pGL3 (Promega) by blunt-end ligation. The resultant plasmid pGL3(ITR) contains the luciferase reporter and head-to-tail ITR element 3′ to the poly(A) site. The integrity of the ITR DNA element within this plasmid was confirmed by partial sequencing and Southern blotting. The persistence of transgene expression from pGL3(ITR) was compared to that of pGL3 by luciferase assays on transiently transfected HeLa cells as described above and analyzed at 10 days (passage 2). Transfection efficiencies were normalized by using a dual renilla-luciferase reporter vector (pRLSV40; Promega).

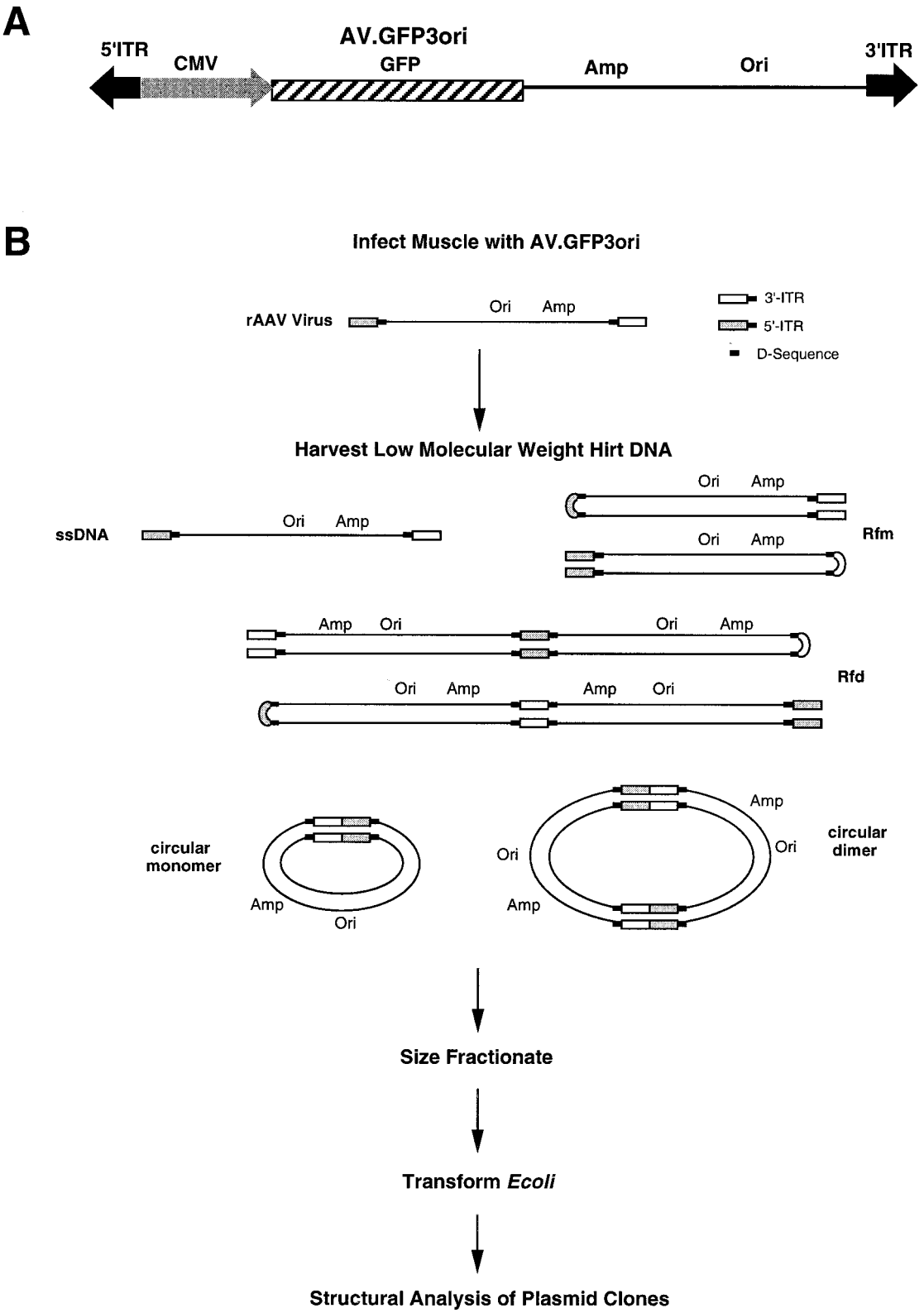

FIG. 1. Isolation of rAAV circular intermediates. With the aid of a rAAV *cis*-acting plasmid, pCisAV.GFP3ori, recombinant AAV virus (AV.GFP3ori) was generated (A). This vector carries a CMV promoter/enhancer, GFP transgene cassette, ampicillin resistance gene (Amp), and bacterial replication origin (Ori). (B) Strategy for isolation of rAAV circular intermediates. ssDNA, single-stranded DNA; Rfm, replication form monomer; Rfd, replication form dimer.

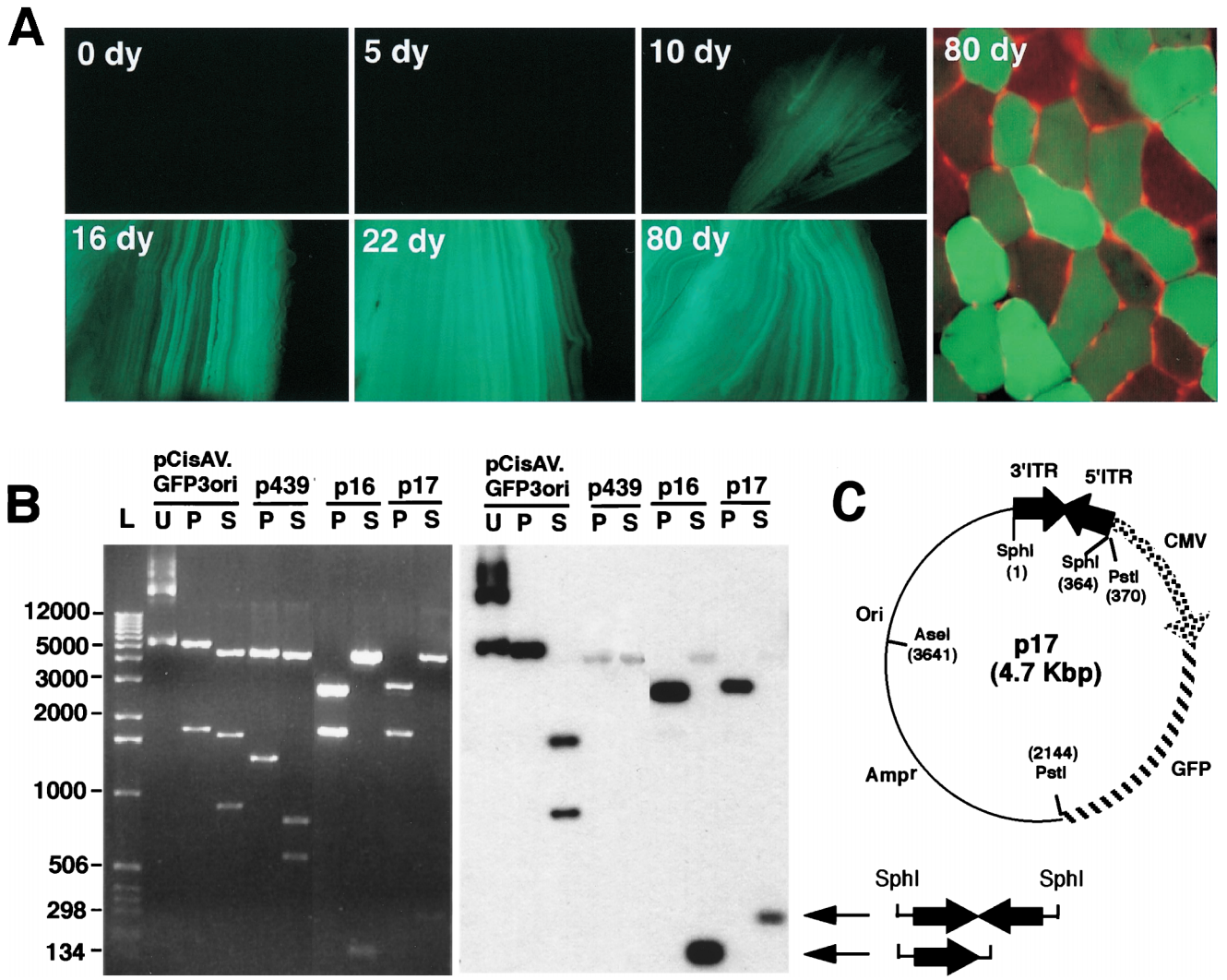

FIG. 2. Formation of rAAV head-to-tail circular intermediates following in vivo transduction of muscle tissue. The tibialis anterior muscles of 4- to 5-week old C57BL/6 mice were infected with AV.GFP3ori (3×10^{10} particles) in HEPES-buffered saline (30 μl). GFP expression (A) was analyzed by direct immunofluorescence of freshly excised tissues and/or in formalin-fixed cryopreserved tissue sections in four independently injected muscle samples harvest at 0, 5, 10, 16, 22, and 80 days (dy) postinfection. GFP expression was detected at low levels beginning at 10 days and was maximum at 22 days postinfection. Expression remained stable to 80 days, at which time more than 50% of the tissue was positive (80-day tissue cross section counterstained with propidium iodide). Hirt DNA was isolated from muscle samples at each of the various time points was used to transform *E. coli*. Rescued plasmids (p439, p16, and p17; all isolated from muscle tissue at 22 days postinfection) were analyzed by Southern blotting (B; agarose gel [left] and ITR-probed blot [right]). Lanes U, uncut; P, *Pst*I cut; S, *Sph*I cut. Positions of molecular weight DNA standards (lane L) are given at the left in base pairs. (C) Schematic drawing of the most predominant type of head-to-tail circular AAV intermediate plasmids rescued from bacteria, showing the structure of p17 as an example (*Sph*I site flanking the 3′ ITR designated the first base pair in the plasmid). Other typical clones included those with fewer than two ITRs as shown for p16. *Sph*I digestion of p16 and p17 plasmids released ITR-hybridizing fragments of approximately 140 and 300 bp, respectively. The slightly lower than predicted apparent molecular size for these ITR fragments (364 bp for an ITR/ITR array) likely represents anomalous migration due to the high secondary structure of inverted repeats within ITRs. Additional restriction enzyme analyses used to determine these structures included double and single digests with *Sph*I, *Pst*I, *Ase*I, and/or *Sma*I (data not shown). Although sequence analysis of p17 and p16 using nested primers to 5′ and 3′ ITRs also confirmed the ITR orientations shown, complete sequence through the central regions of inverted ITR arrays in p17 and similar structures was not possible due to the high secondary structure. Hence, at present it is impossible to rule out the possibility of small deletions in the central junctional regions of inverted ITRs. An example of an atypical clone (p439) rescued from bacteria with unknown structure is also shown.

RESULTS

AAV circular intermediates represent stable episomal forms of viral DNA associated with long-term persistence of transgene expression in muscle tissue. To evaluate the molecular characteristics of rAAV genomes in muscle tissue, we used a rAAV shuttle viral vector (AV.GFP3ori) harboring an ampicillin resistance gene, bacterial origin of replication, and GFP reporter gene (Fig. 1A). This recombinant virus was used to evaluate the presence of circular intermediates by bacterial rescue of replication-competent plasmids (Fig. 1B). In these studies, delivery of AV.GFP3ori (3×10^{10} particles) to the tibialis muscles of mice led to GFP transgene expression which peaked at 22 days and remained stable for at least 80 days (Fig. 2A). These results confirmed previous successes in rAAV-mediated gene transfer to muscle tissue (5, 10, 15, 19, 34). The formation of circular intermediates was evaluated by *E. coli* transformation of Hirt DNA harvested from muscle tissue at 0, 5, 10, 16, 22, and 80 days after infection with AV.GFP3ori. In these muscle samples, circular intermediates were found to have a characteristic head-to-tail structure. The most abundant form

included two inverted ITRs within a circularized genome (Fig. 2B, clone p17); also detected was a less frequent form (<5%) of circular intermediates, p439, with undetermined structure. When this type of replication-competent plasmid was seen, it was not included in the quantification of head-to-tail circular intermediates since its structure could not be conclusively determined. The total abundance of muscle Hirt-derived head-to-tail circular intermediates (with one to two ITRs) demonstrated a time-dependent increase that peaked with transgene expression at 22 days and decreased slightly by day 80 (Fig. 3A). Increased diversity in the length of ITR arrays within circular intermediates was seen at longer time points. For example, Fig. 3B demonstrates several isolated circular intermediates with one to three ITRs isolated from 80 days muscle Hirt samples, in contrast to the more uniform structure of circular intermediates with two ITRs in a head-to-tail conformation at 5 to 22 days postinfection (data not shown).

To evaluate the potential for artifactual rescue of linear rAAV genomes by recombination in bacteria, several control experiments were performed. First, uninfected control muscle Hirt DNA preparations, spiked with an equal amount of rAAV used for in vivo infection of muscles, failed to give rise to replicating plasmids following transformation of *E. coli*. Second, when a blunted linear double-stranded *Hin*dIII/*Pvu*II fragment isolated from pCisAV.GFP3ori (encompassing the entire rAAV genome) was used to transform bacteria, no ampicillin-resistant bacterial colonies were obtained. The addition of T4 ligase to this fragment, however, led to significant numbers of bacterial colonies. Third, when purified single-stranded rAAV DNA was used for transformation, no bacterial colonies were obtained. As summarized in Table 1, control experiments clearly demonstrate that linear double-stranded or single-stranded DNA does not transform *E. coli* and that circularization is necessary for transformation. Hence, in vivo circularization of rAAV genomes is a prerequisite for rescuing autonomously replicating plasmids in *E. coli* with this shuttle vector.

Molecular weight of circular intermediates suggest a conversion from monomer to multimer forms over time. To further characterize the circular intermediates isolated from muscles, Hirt samples from 22- and 80-day postinfection muscles were size fractionated by continuous-flow gel electrophoresis (Bio-Rad) prior to amplification in bacteria. As shown in Fig. 4, the majority of circular intermediates at 22 days postinfection comigrated in their native unamplified form with linear double-stranded DNA standards of less than 3 kbp. Very few clones were isolated from fractions of 3 to 5 kbp, and no clones were obtained from fractions larger than 5 kbp, at this time point. Furthermore, this size-fractionated molecular weight of in vivo Hirt DNA-derived circular intermediates at 22 days postinfection correlated with that of head-to-tail monomer undigested circular intermediate plasmids rescued in bacteria from this same time point (~2.5 kbp), suggesting that these native circular genomes may be supercoiled and/or single-stranded DNA molecules. However, it should be noted that although 22-day circular AAV genomes migrated at a native molecular size of <3 kbp as unamplified Hirt DNA, the majority of rescued circular intermediate plasmids from these fractions had linear molecular sizes of 4.7 kbp when digested to completion with the single cutter *Ase*I. In summary, these data suggest that at early time points postinfection in muscle tissue, the predominant form of circular intermediates likely occurs as monomer head-to-tail genomes. The lower apparent molecular size of this fraction compared to replication-form monomer (Rfm; 4.7 kbp) and dimer (Rfd; 9.4 kbp) genomes provides indirect evidence that these forms are not responsible for rescued plasmids in these Hirt DNA samples. Interestingly, when 80-day

FIG. 3. Frequency of circular intermediate formation in muscle tissue following transduction with rAAV. Hirt DNAs isolated from rAAV-infected tibialis muscle samples were used to transform *E. coli*, and the rescued plasmids were analyzed by Southern blotting as previous described (more than 20 clones were analyzed from at least two independent muscle samples for each time point). (A) Numbers (mean ± standard error) of total head-to-tail circular intermediate clones (line) and total ampicillin-resistant bacteria clones (bar) isolated from each tibialis anterior muscle at 0, 5, 10, 16, 22, and 80 days postinfection. Only plasmids which contained one to two ITRs were included in the estimation of total head-to-tail circular intermediates. Plasmids which demonstrated an absence of ITR-hybridizing *Sph*I fragments (between 150 to 300 bp) were omitted from the calculations. (B) Diversity of ITR arrays found in head-to-tail circular intermediates at 80 days postinfection. The Southern blot was probed with ITR sequences and represents circular intermediates with one to three ITRs. *Sph*I fragments which excise the inverted ITR arrays and hybridize to ITR probes are marked by arrowheads at the right. Sizes of molecular weight standards are indicated at the left in base pairs. Additional restriction enzyme analysis was used to determine the structure of monomer and multimer circular intermediates. Examples are shown for two multimer circular intermediates (p136 and p143) which contain approximately three AAV genomes. Undigested p136 and p143 plasmids migrate at >12 kbp whereas the predominant forms of head-to-tail undigested circular intermediates at 22 days migrate at 2.5 kbp (data not shown). The digestion pattern of p136 is consistent with a uniform head-to-tail configuration of three genomes and is indistinguishable from the digestion pattern of p139, which contains one circularized genome (undigested p139 migrates at 2.5 kbp [data not shown; also see results for p17 in Fig. 2]). In contrast, p136 exhibits a more complex head-to-tail multimer circular intermediate which has various deletions and duplications within the ITR arrays. (C) Predicted structures of five representative intermediates (complete data for structural analysis are not given).

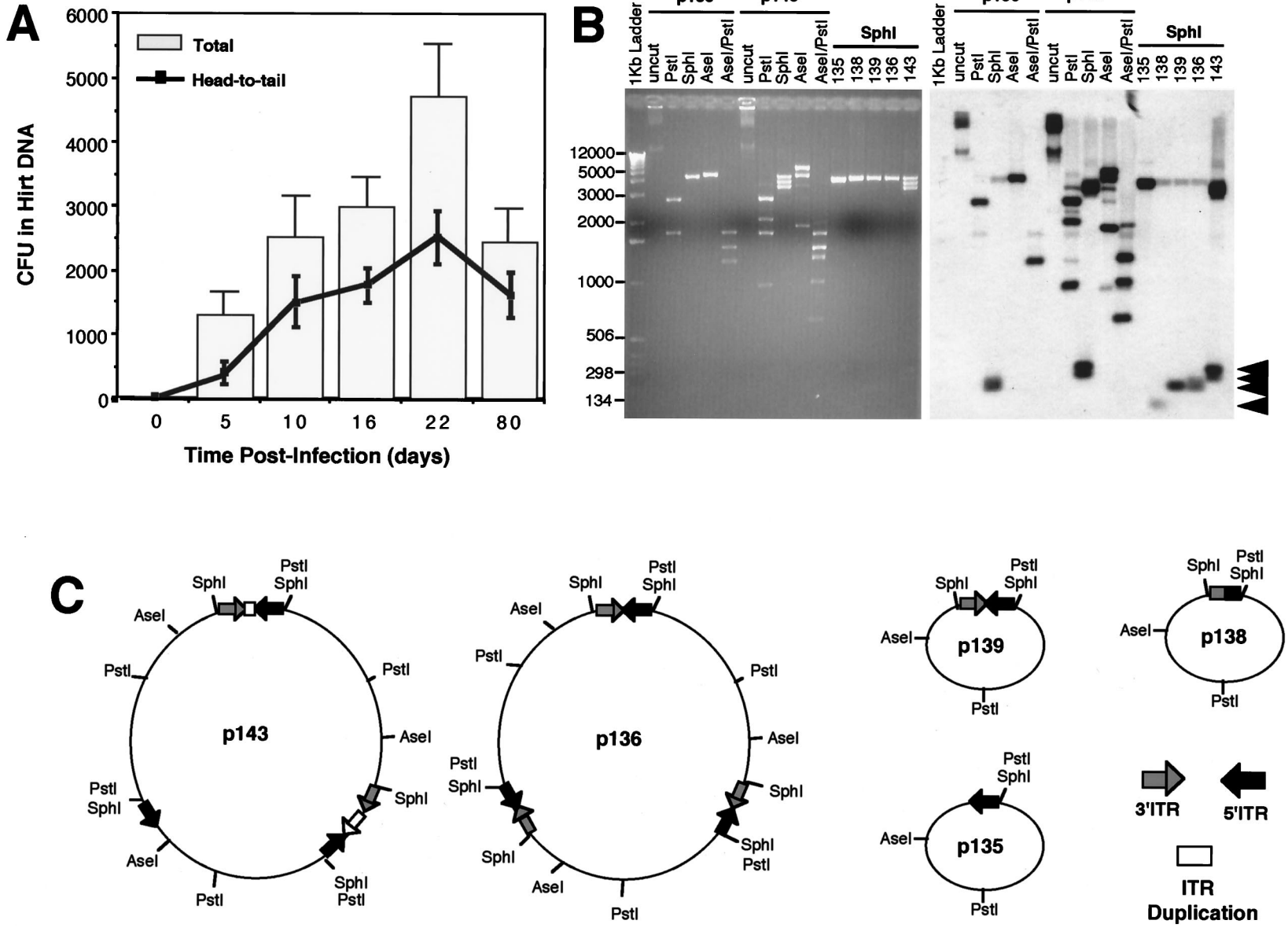
A
CFU in Hirt DNA
Total
Head-to-tail
6000
5000
4000
3000
2000
1000
0
0
5
10
16
22
80
Time Post-Infection (days)
B
1Kb Ladder
p136
p143
uncut
PstI
SphI
AseI
AseI/PstI
SphI
135
138
139
136
143
12000
5000
3000
2000
1000
506
298
134
C
p143
p136
p139
p138
p135
PstI
SphI
AseI
3'ITR
5'ITR
ITR
Duplication

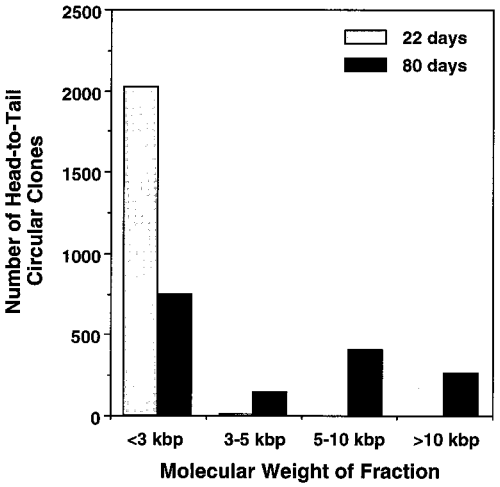

FIG. 4. Molecular sizes of native unamplified circular intermediates in muscle tissue. Hirt DNA from AV.GFP3ori-infected muscle was size fractionated by electrophoresis, and fractions of various molecular weights were transformed into *E. coli*. Results demonstrate the abundance of head-to-tail circular intermediates at each of the given molecular sizes at 22 and 80 days after infection with the rAAV shuttle vector. Fractions were sized according to the migration of linear double-stranded DNA standards under identical gel running conditions. The structures of circular intermediates were confirmed by Southern blot restriction analysis (data not shown).

muscle Hirt DNA samples were size fractionated, more clones were retrieved from larger fractions ranging from 3 to 12 kbp (Fig. 4). This shift in the molecular size of unamplified circular intermediates indicates the potential for recombination between monomer forms in the generation of large circular multimer genomes. Such concatemerization has been previously observed in muscle tissue and has usually been hypothesized to involve linear integrated forms of the AAV genome (5, 10, 15, 34). Our present data shed new light on the molecular characteristics of these persistent AAV genomes and suggest that they are in fact circular and episomal. Based on yields of retrievable circular plasmids reconstituted in Hirt DNA, the efficiency of bacterial transformation, and the initial inoculum of virus, we estimate that approximately 1 in 400 viral DNA particles circularizes following infection in muscle (Table 2). Given the facts that (i) not all rAAV particles likely contain functional DNA molecules, (ii) circular intermediates may integrate, (iii) circular intermediates concatemerize over time, and (iv) transformation efficiencies compared supercoiled plasmid standards to intermediates with an unknown relaxation state, these theoretical calculations may represent an underestimation.

AAV circular intermediates demonstrate increased persistence as plasmid-based vectors. Based on the finding that circular AAV intermediates were associated with long-term persistence of transgene expression in muscle tissue, we hypothesized that rAAV circular head-to-tail intermediates may be molecular structures of the AAV genome associated with the latent life cycle and increased episomal stability. Several aspects of the structure of AAV circular intermediates may account for their increased stability in vivo. First, circularization of AAV genomes may create a nuclease-resistant conformation. Second, since the only viral sequences contained within circular intermediates are the head-to-tail ITR array, these sequences might bind cellular factors capable of stabilizing these structures in vivo. Several studies demonstrating increased persistence of transgene expression with plasmid DNA encoding viral ITRs lends support to this hypothesis (25, 32). We now propose a functional explanation for this finding through the association with circular intermediate formation as part of the AAV life cycle.

To more closely evaluate the persistence of AAV head-to-tail circular intermediates, we performed several in vitro experiments by transfecting these intermediates into HeLa cells and assessing the stability of plasmid DNA and transgene expression by GFP clonal expansion. Results from HeLa cell transfection experiments demonstrated that two monomer head-to-tail circular intermediates (p81 and p87, identical in structure to p139 [Fig. 4C]) studied gave rise to a 10-fold-higher number of 5- and 10-day transgene-expressing clones compared to a control plasmid, pCMVGFP, lacking the ITR sequences (Fig. 5A and B). Additionally, the GFP-positive colonies at 5 days posttransfection were threefold larger in HeLa cells transfected with p81 and p87 than in cells transfected with the pCMVGFP control vector (Fig. 5A and B). These studies suggest the AAV circular intermediates have increased stability of transgene expression and substantiate findings for muscle tissue. However, from the above data, we cannot rule out potential ITR enhancer effects on transgene expression from circular intermediates. Of interest in this regard were two additional findings from these studies. First, the increased transgene expression from AAV circular intermediates p81 and p87 was also immediately apparent by 2 days posttransfection in unpassaged HeLa cells (data not shown). Second, no differences in the persistence of transgene expression were seen among any of the three constructs analyzed in 293 cells (data not shown). These findings suggested that cell-specific factors may mediate increased transcription and/or increased stability of AAV circular intermediates.

To determine whether increases in the persistence of transgene expression correlated with increased molecular persistence of head-to-tail circular intermediates following transfection into HeLa cells, total DNA (low and high molecular weight) was isolated from cultures of pCMVGFP- and p81-transfected HeLa cells at various passages posttransfection and analyzed by Southern blotting. Southern blots hybridized to ^{32}P-labeled GFP probes demonstrated a significantly higher level of p81

TABLE 2. Yield of circular intermediates isolated from Hirt DNA

Bacterial transformation	Starting no. of plasmid or AAV genome molecules	Actual no. of ampicillin-resistant CFU	Adjusted yield (CFU) for 3×10^{10} molecules
Hirt DNA from rAAV-infected muscle[a]	3×10^{10}	5×10^{3}	5×10^{5}[e]
Hirt DNA + 10 ng of LacZ plasmid[b]	1.3×10^{9}	8.7×10^{4}[c]	2×10^{8}[d]
10 ng of LacZ plasmid	1.3×10^{9}	8.7×10^{6}	2×10^{8}[d]

[a] The actual amount of Hirt DNA used for transformation was 3/20 the entire Hirt DNA. The numbers have been adjusted to reflect viral inoculum and yields for the entire muscle.

[b] Plasmid DNA was spiked into mock-infected muscle homogenates prior to isolation of Hirt DNA. This reconstituted Hirt DNA was then used for transformation of bacteria.

[c] The average of several experiments indicates an approximate 100-fold reduction in the number of CFU recovered from bacterial transformations with DNA isolated from Hirt extract spiked with plasmids compared to transformation with an equivalent amount of plasmid DNA alone.

[d] The number of CFU in plasmid reconstitution studies have been adjusted to normalize the number of plasmids genomes to that used in AAV experiments (3×10^{10}). Control LacZ plasmid was approximately 7,000 bp with a molecular size of 4.6×10^{6} g/mol. Therefore, 230 ng of plasmid is equivalent to 3×10^{10} molecules (i.e., normalization factor of 23-fold).

[e] Adjusted yield indicates that approximately 1 in 400 AAV genomes circularizes in vivo.

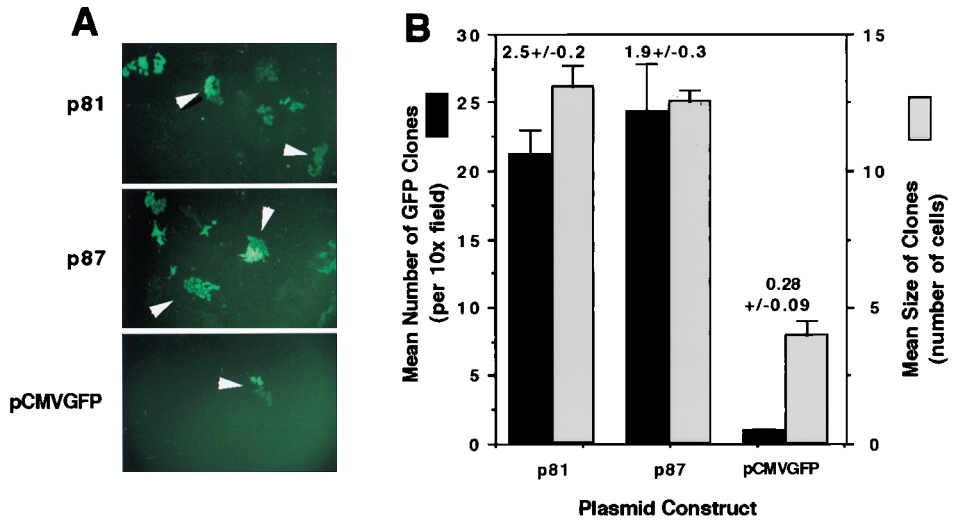

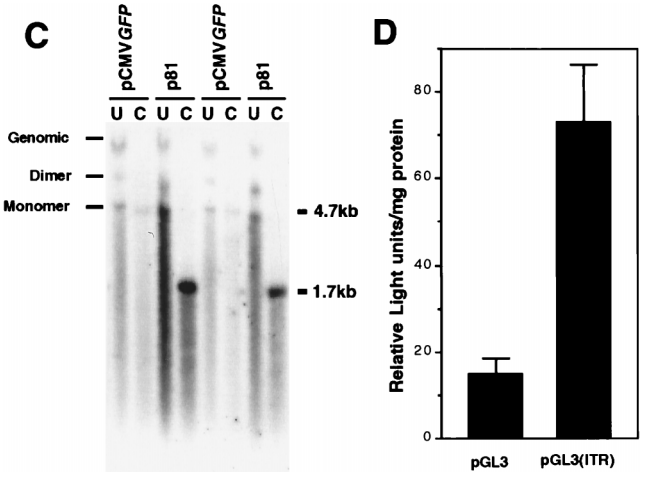

FIG. 5. Head-to-tail circular intermediates demonstrate increased stability of GFP expression following transient transfection in HeLa cells. Subconfluent monolayers of HeLa cells were cotransfected with p81, p87, or pCMVGFP and pRSVlacZ as an internal control for transfection efficiency as described in Materials and Methods. (A) Expansion of GFP clones after one passage (arrowheads). (B) Quantification of clone size (mean raw values) and clone numbers (normalized for transfection efficiency as determined by X-Gal staining for pRSVlacZ). Numbers above the bars represent quantification of GFP clones after passage 2 (also normalized for transfection efficiency). Results indicate the means (± standard errors) of duplicate experiments, with more than 20 fields quantified for each experimental point. The persistence of transfected p81 and pCMVGFP plasmid DNA at passage 7 posttransfection was evaluated by genomic Southern blotting of total cellular DNA hybridized against a ^{32}P-labeled GFP probe (C; results from two independent transfections are shown). In these studies, control cultures cotransfected with pRSVlacZ demonstrated a less than 25% variation in transfection efficiency, as determined by X-Gal staining of cells at 48 h posttransfection. Lanes: U, uncut; C, *Pst*I cut. The migration of uncut dimer and monomer plasmids forms are marked on the left. *Pst*I digestion of the plasmids results in bands at 4.7 kb (pCMVGFP; single *Pst*I site in plasmid) and 1.7 kb (p81; two *Pst*I sites flanking the GFP gene). The band marked Genomic in undigested lanes was also seen with DNA from untransfected cells (data not shown) and hence is nonspecific hybridization of probe to the high concentration of DNA in this area of the gel. To determine whether the head-to-tail ITR array within circular intermediates was responsible for increases in the persistence of GFP expression, the head-to-tail ITR DNA element was subcloned into the luciferase plasmid pGL3 to generate pGL3(ITR). (D) Luciferase transgene expression following transfection with pGL3 and pGL3(ITR) at 10 days (passage 2) posttransfection. Results are the means (± standard errors) for triplicate experiments and are normalized for transfection efficiency by using a dual renilla-luciferase reporter vector (pRLSV40; Promega).

plasmid DNA at passage 7 than that of the control vector lacking the head-to-tail ITR sequence (Fig. 5C). The majority of signal in undigested DNA samples was associated with a 4.7-kb band migrating at the approximate size of the uncut monomer plasmids. Together with the fact that the majority of signal from all cell cultures in Fig. 5C disappeared by passage 10 (data not shown), these data suggest that these plasmids predominantly remained episomal. Thus, in both muscle and HeLa cells, increased persistence of AAV circular intermediates is correlated with stable transgene expression.

ITR arrays are responsible for increased persistence. To investigate whether the head-to-tail ITR DNA element was responsible for the increased persistence of circular intermediates, we cloned this DNA element into a secondary luciferase vector (pGL3) to give rise to pGL3(ITR). Transient transfection experiments in HeLa cells demonstrated a fivefold increase in the persistence of luciferase expression from pGL3 (ITR) compared to that of pGL3 in serially passaged 10 day cultures (Fig. 5D). These findings support the hypothesis that the head-to-tail ITR DNA element contained within circular intermediates is responsible for mediating the increased persistence of transgene expression and suggest a mechanism by which these molecular intermediates may confer stability to AAV genomes in vivo. Furthermore, increases in the stability of transgene expression conferred by this element appear to be primarily context independent, since the head-to-tail ITR element was 3′ to the luciferase gene in pGL3(ITR) and 5′ to the GFP transgene in AAV circular intermediates.

DISCUSSION

Characterization of integrated proviral structures in different cell lines has demonstrated head-to-tail genomes as a predominant structural form following rAAV infection (4, 7). Although head-to-head and tail-to-tail integrated structures have been noted for rAAV (23), these structures are traditionally thought to be associated with wtAAV lytic replication intermediates. These replication intermediates, termed Rfm and Rfd, consist of genomes in duplex monomer and duplex dimer forms, respectively, with one covalently closed end (Fig. 1). Rfd genomes have a characteristic head-to-head or tail-to-tail orientation. Both Rfm and Rfd configurations have also been demonstrated in rAAV-infected cells, and enhanced conver-

sion of single-stranded AAV genomes to double-stranded Rfm and Rfd forms has been suggested as a mechanism for augmentation of rAAV transduction by adenovirus in cell lines (8, 9). However, it is plausible that the mechanisms responsible for the formation of Rfm and Rfd molecules are different from pathways which lead to long-term transgene expression. In support of this hypothesis is a recent study evaluating augmentation of rAAV transgene expression by adenovirus in the liver (30); the results demonstrated that coinfection of the liver with adenovirus and rAAV enhances short-term transgene expression, while long-term expression was no different from that after infection with rAAV alone. The exact mechanism for the formation of head-to-tail circular intermediates is not clear; however, similar structures have been demonstrated to act as preintegration intermediates for retrovirus (31). In this regard, circularized retroviral genomes with one and two viral long terminal repeats have been proposed. In addition, circular preintegration intermediates have also been suggested by recent studies on wtAAV integration (22). The demonstration that circular intermediates exist in rAAV-infected muscle tissue explains several features of latent-phase infection with rAAV vectors, including proviral structure and stable episomal persistence.

Previous studies have suggested that rAAV genomes delivered to muscle tissue might persist as head-to-tail concatemers (5, 10, 15). However, it is not known whether these concatemers exist as free episomes or as integrated proviruses in the host genome. Our results demonstrating prolonged persistence of head-to-tail circular intermediates at 80 days postinfection suggest that a large percentage of rAAV genomes may remain episomal. The conversion of monomer circularized genomes to larger circularized multimers appears to be an aspect associated with long-term persistence and likely represents recombinational events between monomer intermediates and/or rolling replication. Although the bacterial rescue strategy was not capable of satisfactorily addressing the size of multimers, our modified approach to size fractionating Hirt DNA prior to bacterial rescue of intermediates lends support to this hypothesis. Additional supportive evidence for increased recombination over time is the finding that greater variability in the length of ITR arrays was observed at longer time points postinfection. For example, at 5 to 22 days the majority of circular intermediates contained two ITRs in a head-to-tail fashion, whereas at 80 days the ITR arrays consisted of one to three ITRs. Such diversity of ITR arrays in muscle tissue infected with AAV has been previously found in studies using PCR approaches (10, 15). In addition, the 30% decline in the abundance of circular intermediates in muscle tissue between 22 and 80 days also supports a hypothesis that these molecular forms of AAV may represent preintegration complexes.

Given the fact that circular intermediates had long-term persistence in muscle tissue, we hypothesized that certain structural features of these intermediates may affect episomal stability of DNA. Previous studies have noted increased persistence of transgene expression from plasmids encoding AAV ITRs (25, 32). However, the physiologic significance of this finding has remained elusive. Our present study demonstrating that the head-to-tail ITR arrays isolated from AAV circular intermediates can confer increased episomal persistence to plasmids following transfection in cell lines gives a mechanistic framework for ITR effects on plasmid persistence. Furthermore, the correlation that AAV circular intermediates have increased persistence in cell lines in vitro lends support to the hypothesis that these structures represent stable episomal forms following rAAV transduction in muscle. Stability of circular intermediates in vivo might be mediated by the binding of cellular factors to Holliday-like junctions in ITR arrays which stabilize or protect DNA from degradation.

However, several observations regarding the increased persistence of transgene expression conferred by circular intermediates in vitro remain to be explained. First, increased persistence of transgene expression from circular intermediates was observed in HeLa but not 293 cells, which suggests that cell-specific factors may bind to the ITR arrays of circular intermediates to mediate functional effects. Second, increased transgene expression from circular intermediates expressing GFP and the ITR array containing luciferase plasmids was noted by 48 h posttransfection in unpassaged HeLa cells, reminiscent of previous findings which suggest that the AAV ITRs have enhancer-like properties (2). It is not known how an immediate increase in transgene expression from AAV circular intermediates could be linked to increased long-term persistence of DNA. However, one hypothesis could posit the binding of cellular proteins to ITR arrays, which sequesters plasmids into subcompartments of the nucleus which are more transcriptionally active and confer an increased level of DNA stability. Furthermore, we cannot rule out the possibility that the ITR arrays act as enhancers which by virtue of enhanced transcriptional activity and bound proteins at this element protect plasmids from degradation or more evenly segregate plasmids to nuclei during mitosis. Despite the lack of a concrete mechanism for increased persistence of transgene expression from circular intermediates, the current data favor some combination of pathways which involve both enhancer-like function and increased DNA stability conferred by head-to-tail ITR elements.

rAAV has been shown to be an efficient vector for expressing transgenes in various tissues and cell types in addition to muscle, such as brain, retina, liver, lung, and hematopoetic cells (3, 6, 12, 14, 17, 20, 24, 30, 33). Despite these advances in the application of rAAV, the mechanisms of in vivo rAAV-mediated transduction and persistence of transgene expression remain unclear. Questions such as those relating to the molecular state of rAAV following in vivo delivery are highly relevant to the clinical application of this viral vector. For example, should rAAV primarily persist as an randomly integrated provirus, the potential for insertional mutagenesis could present a major theoretical obstacle in the use of this vector due to the potential for mutational oncogenesis. Our demonstration that rAAV can persist as episomes suggests that random integration and associated risks of malignancy may not be a major concern for this viral vector system. Additionally, the molecular determinants of AAV circular intermediates associated with increased persistence in cell lines appear to be contained within the DNA elements encompassing the inverted ITRs. The isolation of this naturally occurring viral DNA element, which forms as part of the AAV life cycle and acts to stabilize circular episomal DNA, may prove useful in increasing the efficacy of both viral and nonviral gene therapy vectors.

ACKNOWLEDGMENT

The work described here was supported by NIH grant R01 DK/HL58340 (J.F.E.).

REFERENCES

1. **Afione, S. A., C. K. Conrad, W. G. Kearns, S. Chunduru, R. Adams, T. C. Reynolds, W. B. Guggino, G. R. Cutting, B. J. Carter, and T. R. Flotte.** 1996. In vivo model of adeno-associated virus vector persistence and rescue. J. Virol. **70:**3235–3241.
2. **Beaton, A., P. Palumbo, and K. I. Berns.** 1989. Expression from the adeno-associated virus p5 and p19 promoters is negatively regulated in *trans* by the Rep protein. J. Virol. **63:**4450–4454.
3. **Bennett, J., D. Duan, J. F. Engelhardt, and A. M. Maguire.** 1997. Real-time,

noninvasive in vivo assessment of adeno-associated virus-mediated retinal transduction. Investig. Ophthalmol. Visual Sci. **38:**2857–2863.
4. **Cheung, A. K., M. D. Hoggan, W. W. Hauswirth, and K. I. Berns.** 1980. Integration of the adeno-associated virus genome into cellular DNA in latently infected human Detroit 6 cells. J. Virol. **33:**739–748.
5. **Clark, K. R., T. J. Sferra, and P. R. Johnson.** 1997. Recombinant adeno-associated viral vectors mediate long-term transgene expression in muscle. Hum. Gene Ther. **8:**659–669.
6. **Conrad, C. K., S. S. Allen, S. A. Afione, T. C. Reynolds, S. E. Beck, M. Fee-Maki, X. Barrazza-Ortiz, R. Adams, F. B. Askin, B. J. Carter, W. B. Guggino, and T. R. Flotte.** 1996. Safety of single-dose administration of an adeno-associated virus (AAV)-CFTR vector in the primate lung. Gene Ther. **3:**658–668.
7. **Duan, D., K. J. Fisher, J. F. Burda, and J. F. Engelhardt.** 1997. Structural and functional heterogeneity of integrated recombinant AAV genomes. Virus Res. **48:**41–56.
8. **Ferrari, F. K., T. Samulski, T. Shenk, and R. J. Samulski.** 1996. Second-strand synthesis is a rate-limiting step for efficient transduction by recombinant adeno-associated virus vectors. J. Virol. **70:**3227–3234.
9. **Fisher, K. J., G. P. Gao, M. D. Weitzman, R. DeMatteo, J. F. Burda, and J. M. Wilson.** 1996. Transduction with recombinant adeno-associated virus for gene therapy is limited by leading-strand synthesis. J. Virol. **70:**520–532.
10. **Fisher, K. J., K. Jooss, J. Alston, Y. Yang, S. E. Haecker, K. High, R. Pathak, S. E. Raper, and J. M. Wilson.** 1997. Recombinant adeno-associated virus for muscle directed gene therapy. Nat. Med. **3:**306–312.
11. **Fisher-Adams, G., K. K. Wong, Jr., G. Podsakoff, S. J. Forman, and S. Chatterjee.** 1996. Integration of adeno-associated virus vectors in CD34+ human hematopoietic progenitor cells after transduction. Blood **88:**492–504.
12. **Flannery, J. G., S. Zolotukhin, M. I. Vaquero, M. M. LaVail, N. Muzyczka, and W. W. Hauswirth.** 1997. Efficient photoreceptor-targeted gene expression in vivo by recombinant adeno-associated virus. Proc. Natl. Acad. Sci. USA **94:**6916–6921.
13. **Flotte, T. R., S. A. Afione, and P. L. Zeitlin.** 1994. Adeno-associated virus vector gene expression occurs in nondividing cells in the absence of vector DNA integration. Am. J. Respir. Cell Mol. Biol. **11:**517–521.
14. **Halbert, C. L., T. A. Standaert, M. L. Aitken, I. E. Alexander, D. W. Russell, and A. D. Miller.** 1997. Transduction by adeno-associated virus vectors in the rabbit airway: efficiency, persistence, and readministration. J. Virol. **71:**5932–5941.
15. **Herzog, R. W., J. N. Hagstrom, S. H. Kung, S. J. Tai, J. M. Wilson, K. J. Fisher, and K. A. High.** 1997. Stable gene transfer and expression of human blood coagulation factor IX after intramuscular injection of recombinant adeno-associated virus. Proc. Natl. Acad. Sci. USA **94:**5804–5809.
16. **Hirt, B.** 1967. Selective extraction of polyoma DNA from infected mouse cell cultures. J. Mol. Biol. **26:**365–369.
17. **Kaplitt, M. G., P. Leone, R. J. Samulski, X. Xiao, D. W. Pfaff, K. L. O'Malley, and M. J. During.** 1994. Long-term gene expression and phenotypic correction using adeno-associated virus vectors in the mammalian brain. Nat. Genet. **8:**148–154.
18. **Kearns, W. G., S. A. Afione, S. B. Fulmer, M. C. Pang, D. Erikson, M. Egan, M. J. Landrum, T. R. Flotte, and G. R. Cutting.** 1996. Recombinant adeno-associated virus (AAV-CFTR) vectors do not integrate in a site-specific fashion in an immortalized epithelial cell line. Gene Ther. **3:**748–755.
19. **Kessler, P. D., G. M. Podsakoff, X. Chen, S. A. McQuiston, P. C. Colosi, L. A. Matelis, G. J. Kurtzman, and B. J. Byrne.** 1996. Gene delivery to skeletal muscle results in sustained expression and systemic delivery of a therapeutic protein. Proc. Natl. Acad. Sci. USA **93:**14082–14087.
20. **Koeberl, D. D., I. E. Alexander, C. L. Halbert, D. W. Russell, and A. D. Miller.** 1997. Persistent expression of human clotting factor IX from mouse liver after intravenous injection of adeno-associated virus vectors. Proc. Natl. Acad. Sci. USA **94:**1426–1431.
21. **Kotin, R. M., R. M. Linden, and K. I. Berns.** 1992. Characterization of a preferred site on human chromosome 19q for integration of adeno-associated virus DNA by nonhomologous recombination. EMBO J. **11:**5071–5078.
22. **Linden, R. M., E. Winocour, and K. I. Berns.** 1996. The recombination signals for adeno-associated virus site-specific integration. Proc. Natl. Acad. Sci. USA **93:**7966–7972.
23. **McLaughlin, S. K., P. Collis, P. L. Hermonat, and N. Muzyczka.** 1988. Adeno-associated virus general transduction vectors: analysis of proviral structures. J. Virol. **62:**1963–1973.
24. **Muzyczka, N.** 1992. Use of adeno-associated virus as a general transduction vector for mammalian cells. Curr. Top. Microbiol. Immunol. **158:**97–129.
25. **Philip, R., E. Brunette, L. Kilinski, D. Murugesh, M. A. McNally, K. Ucar, J. Rosenblatt, T. B. Okarma, and J. S. Lebkowski.** 1994. Efficient and sustained gene expression in primary T lymphocytes and primary and cultured tumor cells mediated by adeno-associated virus plasmid DNA complexed to cationic liposomes. Mol. Cell. Biol. **14:**2411–2418.
26. **Ponnazhagan, S., D. Erikson, W. G. Kearns, S. Z. Zhou, P. Nahreini, X. S. Wang, and A. Srivastava.** 1997. Lack of site-specific integration of the recombinant adeno-associated virus 2 genomes in human cells. Hum. Gene Ther. **8:**275–284.
27. **Rutledge, E. A., and D. W. Russell.** 1997. Adeno-associated virus vector integration junctions. J. Virol. **71:**8429–8436.
28. **Samulski, R. J., L. S. Chang, and T. Shenk.** 1989. Helper-free stocks of recombinant adeno-associated viruses: normal integration does not require viral gene expression. J. Virol. **63:**3822–3828.
29. **Samulski, R. J., L. S. Chang, and T. Shenk.** 1987. A recombinant plasmid from which an infectious adeno-associated virus genome can be excised in vitro and its use to study viral replication. J. Virol. **61:**3096–3101.
30. **Snyder, R. O., C. H. Miao, G. A. Patijn, S. K. Spratt, O. Danos, D. Nagy, A. M. Gown, B. Winther, L. Meuse, L. K. Cohen, A. R. Thompson, and M. A. Kay.** 1997. Persistent and therapeutic concentrations of human factor IX in mice after hepatic gene transfer of recombinant AAV vectors. Nat. Genet. **16:**270–276.
31. **Varmus, H. E.** 1982. Form and function of retroviral proviruses. Science **216:**812–820.
32. **Vieweg, J., D. Boczkowski, K. M. Roberson, D. W. Edwards, M. Philip, R. Philip, T. Rudoll, C. Smith, C. Robertson, and E. Gilboa.** 1995. Efficient gene transfer with adeno-associated virus-based plasmids complexed to cationic liposomes for gene therapy of human prostate cancer. Cancer Res. **55:**2366–2372.
33. **Walsh, C. E., A. W. Nienhuis, R. J. Samulski, M. G. Brown, J. L. Miller, N. S. Young, and J. M. Liu.** 1994. Phenotypic correction of Fanconi anemia in human hematopoietic cells with a recombinant adeno-associated virus vector. J. Clin. Investig. **94:**1440–1448.
34. **Xiao, X., J. Li, and R. J. Samulski.** 1996. Efficient long-term gene transfer into muscle tissue of immunocompetent mice by adeno-associated virus vector. J. Virol. **70:**8098–8108.
35. **Yang, C. C., X. Xiao, X. Zhu, D. C. Ansardi, N. D. Epstein, M. R. Frey, A. G. Matera, and R. J. Samulski.** 1997. Cellular recombination pathways and viral terminal repeat hairpin structures are sufficient for adeno-associated virus integration in vivo and in vitro. J. Virol. **71:**9231–9247.